

Exploring the validity of time-concentration superposition in glassy colloids: Experiments and simulations

Xiaoguang Peng,¹ J. Galen Wang,^{2,3} Qi Li,¹ Dongjie Chen,¹ Roseanna N. Zia,^{3,*} and Gregory B. McKenna^{1,†}

¹Department of Chemical Engineering, Texas Tech University, Lubbock, Texas 79409, USA

²Sibley School of Mechanical and Aerospace Engineering, Cornell University, Ithaca, New York 14853, USA

³Department of Chemical Engineering, Stanford University, Stanford, California 94305, USA



(Received 1 March 2018; revised manuscript received 17 October 2018; published 6 December 2018)

Superposition approaches have generally been proposed to create a dynamic rheological map to access colloidal glassy dynamics beyond experimental time windows. However, the validity of the superposition approaches in colloids near the glass transition is questionable owing to the well-known emergence of a β -relaxation process there. Here, we employ a time-concentration superposition (TCS) approach, analogous to time-temperature superposition and TCS approaches in molecular systems, utilizing a combination of macroscopic rheological experiments and microscopic Brownian dynamics simulations, where concentration jumps are performed by a sudden growth of particle size [soft polystyrene-poly (*N*-isopropylacrylamide) particles in experiment and nearly hard spheres in simulation] at a fixed number of particles. We have examined whether a characteristic master curve can be obtained through horizontal and vertical shifting of the dynamic data, finding that TCS does not hold for either the experimental or simulation systems. We identify the origin of this breakdown as not only the emergence of a strong β -relaxation process but also its overlap with the α relaxation in both the experimental soft-sphere and the simulated nearly hard-sphere colloids near the glass transition concentration. Further understanding of the lack of validity of TCS results from analysis of both experimental and simulation data in the framework of the Baumgaertel-Schausberger-Winter (BSW) relaxation spectrum which provide a means to determine the concentration dependences of both the α and the β relaxations, which seem to follow TCS themselves.

DOI: [10.1103/PhysRevE.98.062602](https://doi.org/10.1103/PhysRevE.98.062602)

I. INTRODUCTION

The physics of the glass transition in condensed soft matter has attracted wide interest in fundamental theory, technology, and application [1–6]. In analogy to the bubble raft model [7–9] utilized to study phase and deformation behavior of metals, colloidal dispersions have been proposed as models to study the dynamic behavior of molecular systems [10,11]. The success of generating colloidal phase diagrams from molecular theories has driven the widely held view that some of the equilibrium mechanisms governing molecular system dynamics may also be valid for colloidal dispersions. One example is the time-temperature superposition (TTS) and time-concentration superposition (TCS) principles in molecular and polymer glass formers, explained as a preservation of structural relaxation modes over all temperatures or concentrations, with only a change in the magnitudes of the relaxation times themselves. Such a simple shifting of the dynamic (relaxation time) spectrum permits construction of broad rheological or dynamical “maps” that extend the range of data beyond that readily obtainable by experiment [12–15]. In these methods the relaxation function (spectrum) shifts uniformly along the time or frequency axis with changing temperature or concentration; i.e., all relaxation modes have

the same qualitative temperature or concentration dependence. In such cases the relaxation times are related through a shift factor $a_T = \tau_i(T)/\tau_i(T_{\text{ref}})$ or $a_\varphi = \tau_i(\varphi)/\tau_i(\varphi_{\text{ref}})$ that is a function of absolute temperature T , or volume fraction φ , obtained by superposing response curves over reference curve but for different temperature or concentration. Here, one curve is arbitrarily selected as the reference curve, and all other curves are shifted to overlap with it; $\tau_i(T_{\text{ref}})$ is the relaxation time for the reference temperature curve, and $\tau_i(T)$ is the relaxation time for the shifted curve. The same procedure is envisioned for relaxation of colloids at different particle volume fraction. In the case of the ideal hard-sphere colloidal system, $\varphi = 4\pi a^3 n/3$, where a is the hydrodynamic particle size set by diffusivity, and n is the number density [12–16]. The shift factors are then scaled relaxation times, meaning that once a superposition is successful the relaxation time at any temperature or concentration can be obtained from the product of shift factor and reference relaxation time at reference temperature or concentration [17]. Such scaling is a powerful method of data treatment not only when it is successful, but perhaps more so when it is not: Any breakdown of the superposition provides information concerning main and secondary relaxations which may individually scale, but when combined results in breakdown of superposition [18–21].

While the use of superposition principles in polymeric systems is widespread, there has been much less exploration of such behavior in colloidal systems [22–29]. In polymeric

*rzia@stanford.edu

†greg.mckenna@ttu.edu

glass formers, the time-temperature superposition or time-concentration superposition principles discussed above have been used as practical and useful tools to construct maps of material dynamics. In colloids there have been some efforts to propose superposition to explore the dynamic behavior and the insight into relaxation mechanisms, particularly close to the glass transition.

The time-concentration superposition (TCS) principle in colloidal systems was exploited by Mattsson *et al.* [26] to determine the concentration dependence of the relaxation time in a series of colloids of different particle hardness. The work resulted in the now well-known observation that “soft colloids make strong glasses” [26]. However, while it is well known that β relaxation emerges at high frequency, the authors focused primarily on the α relaxation, missing an important opportunity to explore the validity of TCS over a fuller range of frequencies. Examination of their full dynamic curves reported in the Supplemental Information of their report reveals another relaxation mechanism that appears at high frequency and at the higher concentrations; while the authors did not recognize this, it suggests to us an important regime where TCS was not investigated. More recently, Archer and co-workers studied soft colloidal particle systems to examine the validity of time-concentration superposition [24,25]. They argued for its validity over a large range of concentrations and very broad (reduced) frequency regime, despite the clear emergence of a high frequency β relaxation. Similar findings have been made for polymeric materials [21], but for time-temperature superposition. Surprisingly, despite substantial study of both soft and hard colloidal systems that exhibit relatively strong relaxations for both the α process and the β process [30–33], we are not aware of any reports specifically demonstrating the failure of TCS. We believe this simple emergence of two independent relaxation modes in itself suggests a potential violation of TCS. The aim of this study is to determine whether a violation of TCS emerges in colloidal glass formers as a result of the emergence of the β relaxation.

In addition, there have been other superposition principles proposed in the domains of both polymer and molecular glasses as well as in colloidal glasses. Hence, full understanding of superposition principles is essential. Though we do not interrogate these other principles in this work, it is worth a brief discussion of them. First, in molecular glasses, there has been some effort to use reduced time concepts in the development of nonlinear constitutive laws. For example, both the Tool-Narayanaswamy-Moynihan (TNM) [34–36] and the Kovacs, Aklonis, Hutchinson, Ramos (KAHR) [37] models of structural recovery rely on time-temperature superposition and time-structure superposition ideas to describe the nonlinear response of glasses that are out of equilibrium. Theories also have been developed with these so-called material clock [38,39] types of models to describe relaxation responses as well as to try to understand yielding and other nonlinear mechanical responses as resulting from stress- or strain-enhanced mobility [40–48]. Many of these models use either stress or strain as parameters that accelerate the molecular dynamics with a fundamental idea underpinning these models of a spectrum of relaxation times that shifts rigidly along the time axis with the change of the stimulus (stress, strain,

temperature, pressure, concentration), without a change in the shape of the spectrum. In the case of colloids, there has been less work in this area, but, for example, Archer and co-workers have proposed that time-strain superposition can describe the mechanical response of colloidal systems [27,28]. At different strains one finds that the responses can be shifted just as if one were working at different temperatures. Also, a recent work by Fielding *et al.* [49] models colloidal deformation response using the strain to accelerate the material time [49]. While it is clear from experiment [50–53] and simulation [54–56] that applied stress or strain seem to accelerate time or increase the molecular or colloidal mobility, caution in all such superposition attempts comes from some work by O’Connell and McKenna in which time-strain superposition was found to describe the relaxation data, but the created master curve was different from that obtained by time-temperature superposition [57].

In addition, strain-rate frequency superposition (SRFS) has been proposed to explore structural relaxation in soft materials [22]. In a typical experiment, a constant strain-rate amplitude is applied to the sample and frequency is varied; i.e., the strain amplitude of the oscillations is varied proportionally to the reciprocal of the frequency. It was found that a master curve could be constructed through vertical superposition. The method and conclusions obtained are, however, problematic because the method results in a violation of the Kramers-Kronig relation relevant to dynamic measurements [23]. Hence, SRFS should be interpreted with caution, though there is recent work on particle filled elastomers that suggest special conditions in which this superposition may be valid [58].

Finally, a method of orthogonal superposition was recently proposed to study the structural relaxation response of colloidal glasses subjected to steady shearing flows [29]. In this instance a dynamic probe is superimposed orthogonally to the shearing plane and apparent storage and loss moduli obtained. The results were interpreted to imply that a time-strain rate mapping could be used to describe the response of the system. Yet, there is a significant body of work that suggests the orthogonal superposition is extremely difficult to interpret. The idea originated in the polymer rheology community [59,60], but there is a consensus in the literature since then that strongly indicates that unambiguous interpretation of such data requires a valid nonlinear constitutive model [61–64]. However, it does appear that the orthogonal superposition is more readily interpreted than is parallel superposition [63,64]. Finally, it is worth noting that in the careful orthogonal superposition work from Jacob *et al.* [29] the superposition seemed valid primarily in the low frequency regime of the orthogonal probe, while in the high frequency regime superposition is at best only approximate.

An important aspect of the present work is that we analyze the data, first, by using simple shifting procedures to observe whether or not time-concentration superposition holds for both investigated systems, then by fitting the data to the empirical Baumgaertel-Schausberger-Winter (BSW) relaxation spectrum [66] we establish the concentration dependences of both the α and β relaxations in addition to establishing whether or not the shapes of the individual mechanisms change as they shift with concentration.

II. EXPERIMENT

A. Synthesis and characterization

A sterically stabilized thermosensitive core-shell PS-PNIPAM [polystyrene-poly (*N*-isopropylacrylamide)] colloid in water was used for the rheological experiments. The thermosensitive core-shell PS-PNIPAM colloids were prepared through a two-step polymerization. The PS core latex containing 5.0 wt% NIPAM was synthesized through emulsion polymerization and the recipe has been described in detail in [67]. The PNIPAM shell was made to have a homogeneous distribution of crosslinker [68], which differs from the previously used method [67,69]. It is formed on the surface of the PS core latex through an *in situ* polymerization: 100 g PS core latex dispersion (8.49 wt% in dried) is loaded into a 500-ml three-neck round bottom flask and diluted with 200 g water under magnetic stirring at 600 rpm. Then 0.109 g *N*, *N'*-methylenebisacrylamide (MBA, 20.0 wt% in total crosslinker) and 3.2 g NIPAM (40.0 wt% in total monomer) are added into the mixture and the mixture is bubbled with nitrogen gas for 45 min. The reaction mixture is heated to 80 °C. The polymerization is initiated by adding 0.166 g potassium persulfate (KPS) dissolved in 20 ml water. After 5 min, a 50-ml solution containing 0.436 g MBA (80.0 wt% in total crosslinker) and 4.8 g NIPAM (60.0 wt% in total monomer) is added continuously into the mixture over 60 min. The reaction is allowed to run for 4 h at 80 °C after completion of the loading steps. The thermosensitive core-shell PS-PNIPAM latexes were purified through dialysis against water for 1 week and the latexes dried at room temperature under vacuum.

The system was chosen owing to the ability to trigger changes in particle size via swelling and deswelling with changes in temperature, as described in [67,69]. The hydrodynamic diameter with a size polydispersity of 18% was measured using dynamic light scattering [70–72] and it can be described with a linear temperature dependence between 22 °C and 32 °C, $D_H(T) = 194.65 - 2.15T$ (T in Celsius, °C), in nanometers, as shown in Fig. 1, consistent with findings from other groups [11,73]. Importantly, the interparticle interactions in PNIPAM dispersions change from repulsive to attractive as temperature increases. However, the transition

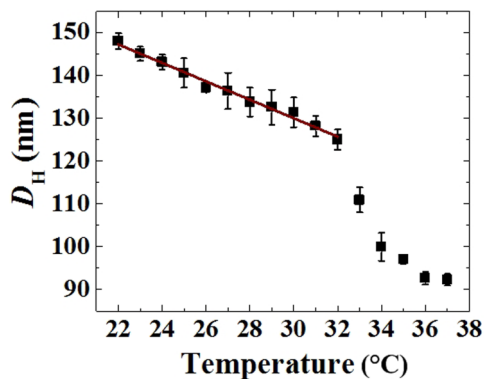


FIG. 1. Temperature dependence of hydrodynamic diameter for the thermosensitive core-shell PS-PNIPAM particle in water, measured using dynamic light scattering (solid line represents the linear equation fit: $D_H(T) = 194.65 - 2.15T$, T in Celsius, °C).

strongly depends on the thickness of the PNIPAM shell [74]. For the present PS-PNIPAM colloidal dispersion, gelation behavior has not been found even at temperatures above the lower critical solution temperature (LCST), consistent with other reports [11,73,75,76]. The repulsive forces from both electrostatic (negative charge from initiator) and steric (from the hairy structure of the PNIPAM) interactions dominate in the PS-PNIPAM system used here. Another relevant point is that the investigated temperature range from 30 °C to 28.2 °C is below the LCST and leads to a particle diameter change of 3%.

The volume fraction of a hard-sphere dispersion can be quantified by the density and mass fraction. However, it is very difficult to determine the thermodynamic volume fraction of soft colloidal dispersions due to the interpenetration and compression of the hairy structure of the PNIPAM shell [30,76]. In the present work the effective volume fraction is used and was calculated at different temperatures based on the hydrodynamic size obtained from dynamic light scattering, and is given by $\varphi_{\text{eff}}(T) = \varphi_{\text{eff}(\text{collapsed})} [D_H(T)/D_{\text{collapsed}}]^3$ [77,78], where $\varphi_{\text{eff}(\text{collapsed})}/\varphi_{\infty}$ is 0.291 at 37 °C and $D_{\text{collapsed}}$ is 92.3 nm. The effective volume fraction of the soft particle dispersion in the collapsed (particle) state was calculated based on the density and mass fraction [77,78], which may underestimate the effective volume fraction due to a small amount of water in the collapsed shell [79,80] even at high temperature. We further remark that the effective volume fraction of the soft colloidal dispersion was also determined from relative viscosity measurements at very low concentrations using the Einstein-Bachelor equation [22,76]. There is a large difference in the effective volume fractions between these two methods, hence a large uncertainty in the true volume fraction of the soft colloidal systems. The effective volume fraction based on the dilute concentration relative viscosity determinations is up to several hundred percent [22,81,82], even though the actual maximum volume fraction cannot exceed unity. Therefore, in analogy to the scaling by T_g or φ_g used in the so-called Angell plot ($\log\tau$ vs T_g/T) for glass-forming systems [30,83], we have scaled the concentrations in this work (both the experimental and the simulations) by the nominal divergence value φ_{∞} determined from a Vogel-Fulcher-Tammann [84–86] type of fitting of the data, as described subsequently. Hence, $(\varphi/\varphi_{\infty})$ is used throughout the work as the scaled concentration. Scaling the volume fraction by φ_{∞} provides a way to scale out the uncertainties in the volume fractions of the soft colloids and relate them to the nominal ideal glass volume fraction. The same scaling with the hard-sphere simulation data provides a means of comparison of the systems at similar “distances” from the glass concentration.

B. Rheological measurements

Rheometry was performed using a stress-controlled rotary rheometer (AR-G2, TA Instruments), equipped with a cone-plate geometry having a diameter of 40 mm and cone angle of 2°. The colloidal sample was surrounded by Krytox oil to prevent solvent evaporation during testing. The rheological measurements were performed after sudden volume fraction increases (up-jumps) from the liquid state at a low volume

fraction to various final high volume fractions, and then aged into an intransient state, where the response became independent of time.

C. Brownian dynamics simulations

Brownian dynamics (BD) simulations of a nearly hard-sphere colloidal dispersion were conducted using the LAMMPS dynamic simulation package [87], with parameters set to recover Stokesian colloidal physics as described previously [87,88]. The colloidal system comprised 55 000 freely draining Brownian spheres with average hydrodynamic radius a . Particles interacted via a nearly hard-sphere Morse potential and a size polydispersity of 7% was applied to avoid crystallization [89]. The system was periodically replicated to model an infinite system. The concentration jumps in the simulations were carried out by performing jumps in particle diameter at a fixed number of particles. Particle positions were monitored throughout each simulation and the mean-square displacement (MSD) computed from these data and evaluated as a function of lag time, where the determinations were made in a sequence of waiting times following the concentration jump. The intransient state was identified as the time at which the MSD became independent of aging time. The volume fraction up-jumps in simulation were performed from the same initial volume fraction of 0.50 to the various final volume fractions which ranged from 0.51 to 0.58. A quench rate of $\frac{d\varphi}{dt} =$

$0.25D/a^2$ was used, where $D = k_B T / 6\pi\eta a$ is the diffusion coefficient of a single colloid of size a in a solvent with viscosity η and a^2/D is the Brownian time t_B . Consequently, it physically takes 0.04 Brownian times to change the volume fraction by 0.01, e.g., from 0.50 to 0.51. After the quench, the colloidal system at each volume fraction was aged for different waiting times and the MSD measured over the lag time until an intransient state was reached, as evidenced by overlapping of the MSD curves with increasing waiting time after the volume fraction jump.

III. RESULTS AND DISCUSSION

A. Experimental section

Figure 2 shows plots of typical rheological data obtained from the dynamic experiments in the present study, following a jump from the liquid state at $\varphi/\varphi_\infty = 0.802$, into the putative glassy region [4,6,10,26,29,30]. Figure 2(a) shows the creep compliance, which exhibits the expected aging response for the PS-PNIPAM colloidal dispersion evolving toward an intransient state after a volume fraction up-jump from an equilibrium state at $\varphi/\varphi_\infty = 0.802$ to $\varphi/\varphi_\infty = 0.885$. Just after the jump, the system has been driven out of equilibrium. The creep compliance curves shift to the right with increasing aging time and eventually overlap with each other, indicating that the intransient state is approached [90]. We

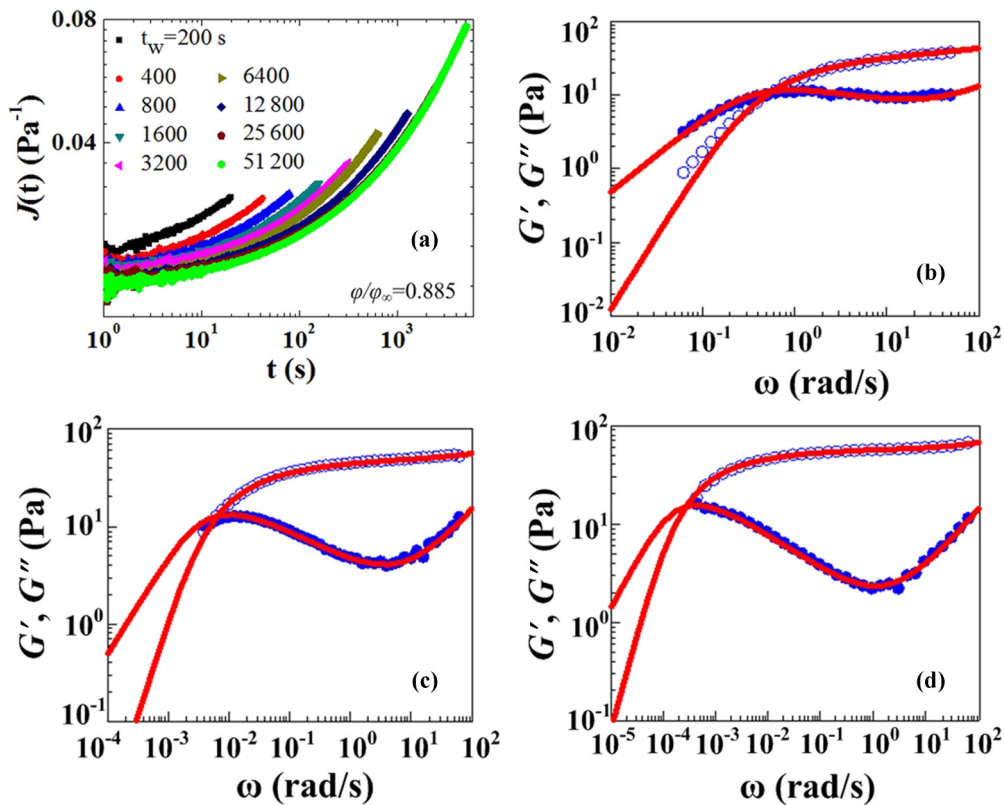


FIG. 2. Experimental results: (a) Creep aging behavior for the PS-PNIPAM colloidal dispersion after volume fraction up-jump from $\varphi/\varphi_\infty = 0.802$ to $\varphi/\varphi_\infty = 0.885$ and then aged into intransient state. The frequency dependence of storage modulus $G'(\omega)$ (open symbols) and loss modulus $G''(\omega)$ (closed symbol) for the PS-PNIPAM colloidal dispersion after volume fraction up-jump from $\varphi/\varphi_\infty = 0.802$ to $\varphi/\varphi_\infty = 0.844$ (b), 0.868 (c), and 0.885 (d), and measured in intransient state (solid lines represent the Baumgaertel-Schausberger-Winter (BSW) relaxation spectrum fitting [66]).

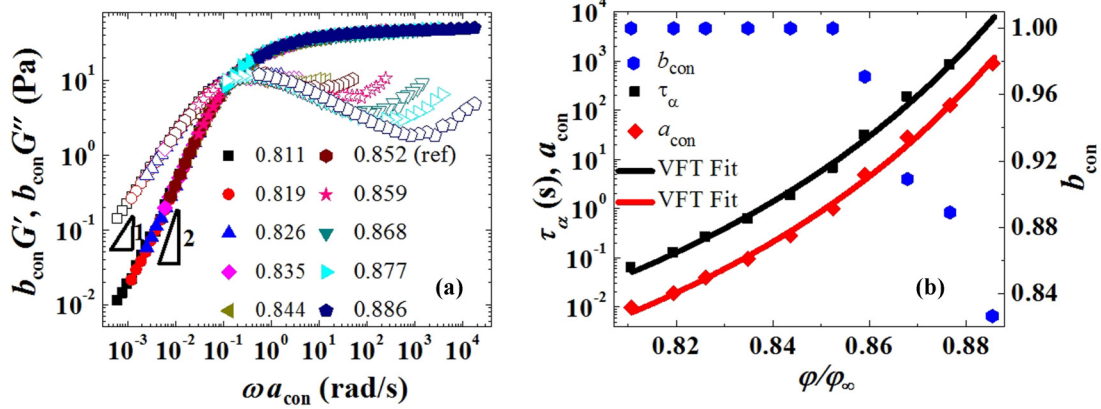


FIG. 3. Experimental results: (a) Time-concentration superposition (TCS) master curve [reduced $G'(\omega)$ (closed symbols) and reduced $G''(\omega)$ (open symbols)] constructed from dynamic data for the PS-PNIPAM colloidal dispersion after volume fraction up-jump perturbations in intransient state and data in Fig. 2. The volume fractions given as φ/φ_∞ are shown in the figure. (b) The relaxation time τ_α (closed squares), concentration dependence of horizontal (a_{con} , closed diamonds) and vertical (b_{con} , closed hexagons) shift factors vs volume fraction for the PS-PNIPAM colloidal dispersion (solid line represents the Vogel-Fulcher-Tammann (VFT) fitting [84–86]).

remark that physical aging occurs at a fixed volume fraction (*iso*-volume fraction condition) for the colloidal dispersions, different from the isobaric and isothermal conditions usually investigated in molecular systems [1,21,91]. Figures 2(b)–2(d) show the frequency dependence of storage modulus $G'(\omega)$ and loss modulus $G''(\omega)$ for systems aged into the intransient state for three different (scaled) volume fractions after up-jumps from $\varphi/\varphi_\infty = 0.802$ to $\varphi/\varphi_\infty = 0.844$, 0.868 , and 0.885 in Figs. 2(b)–2(d), respectively. The crossover point where $G'(\omega)$ equals $G''(\omega)$ shifts to lower frequency with increasing volume fraction, and the relaxation time τ_α [$\tau_\alpha = 1/\omega$ at $G'(\omega) = G''(\omega)$] becomes longer as crowding slows dynamics. Another point of interest is that with increasing volume fraction, a plateau develops in $G'(\omega)$ and is accompanied by a minimum in $G''(\omega)$, typical of glass-forming colloids [10,11,29].

Analogous to TTS in molecular systems, if a time-concentration superposition (TCS) is valid, a master curve should emerge upon shifting the data in Fig. 2 by scalar shift factors a_{con} and b_{con} to give reduced storage modulus $b_{\text{con}}G'(\omega a_{\text{con}})$ and reduced loss modulus $b_{\text{con}}G''(\omega a_{\text{con}})$, where the subscript “con” denotes the concentration jump. The results of such shifting are plotted in Fig. 3(a). The master curve was constructed by horizontal shifting of the dynamic data to a reference curve at volume fraction $\varphi/\varphi_\infty = 0.852$. Vertical shifting was also needed and the vertical shift factors b_{con} are reported in Fig. 3(b). In the low frequency terminal region, the data in Fig. 3(a) fall on a single master curve and the reduced $G'(\omega)$ and $G''(\omega)$ are proportional to (reduced) frequency with a scaling relationship: $G''(\omega) \sim \omega^1$ and $G'(\omega) \sim \omega^2$, following a typical Maxwellian behavior [16]. In contrast, while the $G'(\omega)$ data seem to superpose over the entire frequency range, it is clear that as volume fraction increases, the crossover regime [region where $G''(\omega)$ exhibits a minimum] in $G''(\omega)$ becomes wider and deeper and the $G''(\omega)$ data do not superimpose. Another point of interest is seen in Fig. 3(b) where the relaxation time τ_α [extracted from the crossover point between $G'(\omega)$ and $G''(\omega)$] is plotted as a function of volume fraction. Typical of the

behavior of glass-forming colloids, τ_α displays a dramatic growth with increasing volume fraction [10,92–94]. The solid curves in the figure show that the volume fraction dependence of τ_α and shift factors a_{con} can be described by a modified Vogel-Fulcher-Tammann (VFT) fit [84–86]: $\log_{10}(\tau_\alpha) = B + C/(\varphi_\infty - \varphi)$, in which $B = -9.126$, $C = 0.6703$, where φ_∞ represents the modified VFT divergent volume fraction and $\varphi_\infty = 0.454$ in this case (see prior comments on volume fraction). Unsurprisingly, as the divergent concentration is approached the relaxation time grows dramatically with increasing volume fraction (approximately five decades in the range here from $\varphi/\varphi_\infty = 0.802$ to $\varphi/\varphi_\infty = 0.885$), consistent with the glasslike behavior of colloids [30].

To gain further insight into the individual relaxation modes and how they vary with concentration, the shape of the dynamic data in Figs. 2(b)–2(d) was analyzed via a Baumgaertel-Schausberger-Winter (BSW) relaxation spectrum or function [66]. The BSW relaxation spectrum was originally proposed to describe dynamic data in the terminal flow and rubbery plateau regions of entangled linear flexible monodisperse (LFM) polymers [66] and is based on an empirical power-law relaxation spectrum expressed in the following simple form [66,95]:

$$H(\tau) = n_\alpha G_N \left\{ \left(\frac{\tau}{\tau_\alpha} \right)^{n_\alpha} + \left(\frac{\tau}{\tau_\beta} \right)^{-n_\beta} \right\}, \quad (1)$$

where H is the relaxation spectrum. Originally, n_α and n_β corresponded to a slope for the spectrum in the entanglement regime and a slope for the spectrum in the transition to the glass, respectively; τ_α and τ_β refer to characteristic times for the system. G_N is a material-specific constant, and taken as the rubbery plateau modulus in the case of the entangled polymers. The storage modulus and loss modulus were obtained from the following equations [66]:

$$G'(\omega) = G_N + \int_0^{\tau_{\text{max}}} \frac{d\tau}{\tau} H(\tau) \frac{(\omega\tau)^2}{1 + (\omega\tau)^2}, \quad (2)$$

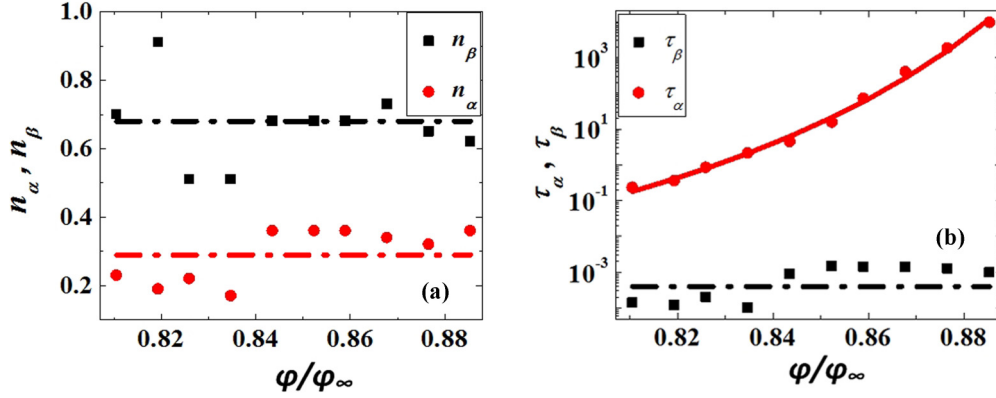


FIG. 4. Experimental results: (a) The BSW function fitting parameters n_α and n_β vs φ/φ_∞ for the PS-PNIPAM colloidal dispersion. (b) The BSW function fitting parameters τ_α and τ_β for the PS-PNIPAM colloidal dispersion. τ_α and τ_β refer to the characteristic times for the system (solid line represents the modified VFT [84–86] fit: $B = -9.126$ and $C = 0.6703$; dashed lines are given as guides to the eye).

and

$$G''(\omega) = \int_0^{\tau_{\max}} \frac{d\tau}{\tau} H(\tau) \frac{(\omega\tau)}{1 + (\omega\tau)^2}. \quad (3)$$

τ_{\max} represents the upper limit of the relaxation time spectrum. The BSW expression has also been successfully used to describe the relaxation response for small molecule glass-forming systems near their glass transition temperature [96] and was recently found to describe the dynamics of concentrated soft colloidal dispersions [32], and successfully captured both the terminal and plateau regions of the glass-forming colloid; i.e., it fit the primary α -relaxation and secondary β -relaxation processes, respectively. In the present study, the solid lines in Figs. 2(b)–2(d) represent the results of fitting a BSW function to our dynamic data for the concentrated colloidal dispersions. We remark that when TTS is valid for molecular systems, it is found that both n_α and n_β are constants independent of temperature while the relaxation times τ_α and τ_β both follow the same temperature dependence [66,95,96]. As seen in Fig. 4(a), for the present colloidal system, both n_α and n_β are nearly independent of volume fraction. This is consistent with the postulation from Winter *et al.* [32] in their work using the BSW function to describe the dynamics of soft colloidal dispersions. In that case, they emphasized the behavior of the n_α parameter and did not report the actual behavior of n_β . Fig. 4(b) shows that the values of τ_α and τ_β that represent the main and secondary relaxation times, respectively, exhibit different volume fraction dependences: τ_α grows dramatically with volume fraction, following a super-Arrhenius glass-like behavior, while τ_β has a negligible dependence on volume fraction. As a result, the combination of different relaxation mechanisms leads to a breakdown of TCS for the full dynamic response of our colloidal dispersions, while the individual mechanisms follow TCS. We remark that the BSW fitting parameter τ_α in Fig. 4(b) shows the same volume fraction dependence as the α relaxation time obtained from the crossover point between $G'(\omega)$ and $G''(\omega)$ [Fig. 3(b)]. Of additional interest in Fig. 4(a), the value of n_β is larger than n_α for the PS-PNIPAM systems, consistent with findings for other systems including polymers and colloids [11,32,66,95,96], although the physical

meaning of this comparison is not yet established. In contrast, the value of n_α is larger than n_β in the mode coupling theory (MCT) prediction [32]. We also remark that the weak to zero dependence of the τ_β on the concentration is similar to qualitative observations from other works [11,30,31,97,98].

B. Simulations

To further examine TCS in colloidal dispersions, Brownian dynamics (BD) simulations were conducted to study the dynamics of a system that has aged into an intransient state after volume fraction up-jumps. The positions of each individual particle can be tracked over time throughout each simulation, and the slowing of particle dynamics carefully monitored as concentration increases. While diffusion has been shown to remain proportional to the inverse of suspension viscosity up to high volume fractions [99–106], the coefficient of proportionality in such a dense, noncontinuum system is not quantitatively obtainable via a generalized Stokes-Einstein relation [89]. Nonetheless one can obtain an estimate via that relation [65]:

$$|G^*(\omega)| \approx \frac{k_B T}{\pi a \langle \Delta r^2(\frac{1}{\omega}) \rangle \Gamma[1 + \alpha(\omega)]}, \quad (4)$$

where k_B is the Boltzmann constant, T is absolute temperature, a is the hydrodynamic radius, Γ is the gamma function, and $\alpha(\omega) = \frac{d \ln \langle \Delta r^2(\frac{1}{\omega}) \rangle}{d \ln(\frac{1}{\omega})}$. The dynamic moduli $G'(\omega)$ and $G''(\omega)$ can, then, be calculated from [65]

$$G'(\omega) = |G^*(\omega)| \cos\left(\frac{\pi\alpha(\omega)}{2}\right) \quad (5)$$

and

$$G''(\omega) = |G^*(\omega)| \sin\left(\frac{\pi\alpha(\omega)}{2}\right). \quad (6)$$

This provides a bridge between experiment and simulation.

Figure 5(a) shows the reduced mean-square displacement (MSD) (averaged over all particles in the system) vs time at different aging times after a volume fraction up-jump from 0.50 ($\varphi/\varphi_\infty = 0.828$) to 0.58 ($\varphi/\varphi_\infty = 0.960$). The simulations capture physical aging behavior similar to that of

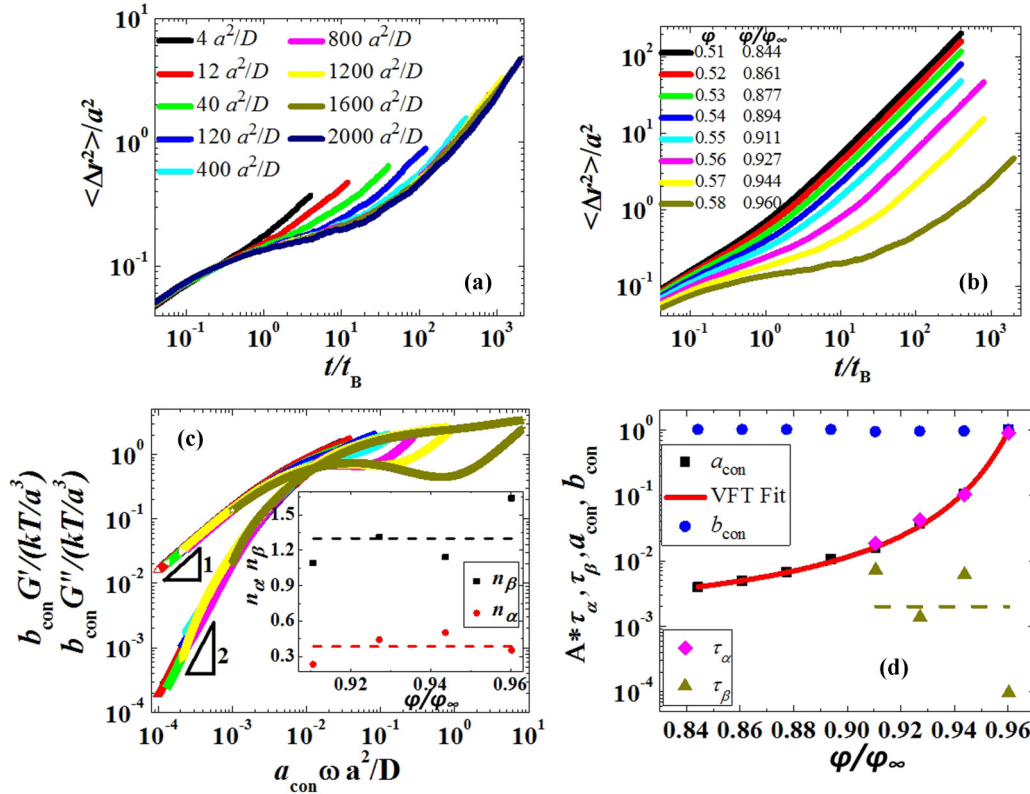


FIG. 5. Dynamic simulations: (a) Reduced mean-square displacement (MSD) vs time from BD simulations for hard-sphere colloidal dispersion after volume fraction up-jump from 0.50 ($\phi/\phi_\infty = 0.828$) to 0.58 ($\phi/\phi_\infty = 0.960$) at different aging times, where t_B is the Brownian time. Note that the angle brackets indicate an ensemble average over all particles in the system. (b) Reduced MSD vs time for colloidal dispersions at different volume fractions in intransient state. (c) Reduced master curve was constructed following TCS and data were obtained from reduced MSD vs time in intransient state via the generalized Stokes-Einstein relation (GSER) [65,67] [reduced $G'(\omega)$ (closed symbols) and reduced $G''(\omega)$ (open symbols)]. Inset: The BSW function fitting parameters n_α and n_β vs ϕ/ϕ_∞ (dashed lines are given as guides to the eye). (d) The concentration dependence of horizontal (a_{con}) and vertical (b_{con}) shift factors and the BSW fitting parameters τ_α and τ_β vs scaled volume fraction (solid line represents the modified VFT fitting [84–86], where $B = -3.219$ and $C = 0.077$). (The coefficient A was applied to superimpose relaxation time τ_α with horizontal factor a_{con} and $A = 0.005$.)

the experimental data displayed in Fig. 2(a): as aging time increases the MSD curves shift to the right until they overlap at the longest time, indicating that the colloidal system has evolved into an intransient state. Figure 5(b) shows the MSD vs time response (in the intransient state) at different final volume fractions, where short- and long-time regimes are evident. At short times, the particles diffuse within a cage of nearest neighbors without disturbing their arrangement. At intermediate times, they exchange places with their neighbors, a correlated motion that produces nonlinear growth in the MSD. As concentration grows, local cages become tight, resulting in the emergence of a plateau; this is commonly considered as the β relaxation [107]. Eventually the particles are able to exchange positions with their neighbors many times even though they may remain close to their original positions; this diffusion corresponds to α relaxation [107]. With increasing volume fraction, the plateau in MSD vs time gets longer. At lower volume fractions, there is no obvious plateau in $G'(\omega)$ nor a minimum in $G''(\omega)$; hence the BSW function is not applicable in this regime because of the limited frequency range available for the lower concentrations. At higher concentrations and analogous to the experimental TCS data treatment, a master curve from the simulated data was

determined and is plotted in Fig. 5(c). The dynamic data for the high volume fractions in the range from 0.55 ($\phi/\phi_\infty = 0.911$) to 0.58 ($\phi/\phi_\infty = 0.960$) can be successfully fitted by the BSW function as the system develops more and more pronounced β relaxation. It is of particular interest that the freely draining BD simulations completely capture the essential experimental findings: The $G''(\omega)$ peak becomes wider and deeper with increasing volume fraction and a single master curve in the dynamic data cannot be obtained through TCS, indicating that TCS does not hold for concentrated colloidal dispersions and that hydrodynamic interactions play a negligible role. Horizontal and vertical shift factors are also plotted in Fig. 5(d). The volume fraction dependence of the horizontal shift factor a_{con} can be described by the modified VFT equation, a super-Arrhenius behavior with $\phi_\infty = 0.604$, $B = -3.219$, and $C = 0.077$. Figures 5(c) and 5(d) show the BSW relaxation spectrum fitting parameters as functions of concentration. The slopes n_α and n_β are nearly independent of the volume fraction, and τ_α and τ_β follow different concentration dependences: τ_α follows a super-Arrhenius glass-like behavior, while τ_β has a weak volume fraction dependence. We remark that the values of n_β are far above unity for the simulation data, consistent with simulation data from the

literature [29] (those simulation data were digitized and fitted using the BSW relaxation spectrum), and higher than those in the experimental data [32]. We postulate that the reasons for the difference originate from the investigated conditions: For the BD simulation, only Brownian motion was considered, while for the experiment the particle softness also plays a role.

IV. CONCLUSIONS

We have examined the validity of time-concentration superposition for colloidal dispersions via experiment and simulation. It is found that time-concentration superposition fails for the investigated concentrated colloidal dispersions due to the development of a strong, high frequency, β -relaxation process which overlaps with the α -relaxation process. A quantitative analysis of the failure of time-concentration superposition was carried out via the Baumgaertel-Schausberger-Winter (BSW) relaxation spectrum. The BSW analysis of the dynamic data suggests that α - and β -relaxation mechanisms, while individually following TCS, show different volume fraction dependences, which, in turn, leads to the breakdown of time-concentration superposition. In addition, Brownian dynamics simulations produced MSD data from which the

moduli were estimated via the generalized Stokes-Einstein relation (GSER). The simulated $G'(\omega)$ and $G''(\omega)$ results successfully capture the experimental behavior of a minimum in $G''(\omega)$ and show that the β relaxation strongly separates from the α relaxation as volume fraction increases, further showing that one cannot achieve a single master curve representation of the data. It is concluded that time-concentration superposition fails for the concentrated colloidal dispersions, as shown here by both experiment and simulation. However, as supported by the BSW analysis, the individual mechanisms are superposable, as frequently found in molecular systems [19,106]. This should be further explored in other colloidal systems to ensure that it is a general behavior.

ACKNOWLEDGMENTS

Support from the National Science Foundation under Grants No. CBET-1133279, No. CBET-1506072, and No. CBET-1506079, and the John R. Bradford endowment at Texas Tech University are acknowledged, each for partial support of this work. We also thank Professor H. H. Winter for providing access to IRIS Software. R.N.Z. also thanks Professor E. R. Weeks for many helpful discussions.

-
- [1] G. B. McKenna, in *Comprehensive Polymer Science*, edited by C. Booth and C. Price (Pergamon, Oxford, 1989), Vol. 2, pp. 311–362.
 - [2] J. Mewis and N. J. Wagner, *Colloidal Suspension Rheology* (Cambridge University Press, Cambridge, 2012).
 - [3] *Dynamical Heterogeneities in Glasses, Colloids, and Granular Media*, edited by L. Berthier, G. Biroli, J. Bouchaud, L. Cipelletti, and W. Van Saarloos (Oxford Science Publications, New York, 2011).
 - [4] P. N. Pusey and W. van Meegen, Phase behaviour of concentrated suspensions of nearly hard colloidal spheres, *Nature* **320**, 340 (1986).
 - [5] K. S. Schweizer and E. J. Saltzman, Entropic barriers, activated hopping, and the glass transition in colloidal suspensions, *J. Chem. Phys.* **119**, 1181 (2003).
 - [6] W. C. K. Poon and P. N. Pusey, in *Observation, Prediction and Simulation of Phase Transitions in Complex Fluids*, edited by M. Baus, L. F. Rull, and J. Ryckaert (Springer, Netherlands, Dordrecht, 1995), pp. 3–51.
 - [7] A. S. Argon and H. Y. Kuo, Plastic flow in a disordered bubble raft (an analog of a metallic glass), *Mater. Sci. Eng.* **39**, 101 (1979).
 - [8] A. W. Simpson and P. H. Hodgkinson, Bubble raft model for an amorphous alloy, *Nature* **237**, 320 (1972).
 - [9] S. L. Bragg and J. F. Nye, A dynamical model of a crystal structure, *Proc. R. Soc. London, Ser. A* **190**, 474 (1947).
 - [10] G. L. Hunter and E. R. Weeks, The physics of the colloidal glass transition, *Rep. Prog. Phys.* **75**, 066501 (2012).
 - [11] M. Siebenbürger, M. Fuchs, H. H. Winter, and M. Ballauff, Viscoelasticity and shear flow of concentrated, noncrystallizing colloidal suspensions: Comparison with mode-coupling theory, *J. Rheol.* **53**, 707 (2009).
 - [12] M. Hu, Y. Xia, G. B. McKenna, J. A. Kornfield, and R. H. Grubbs, Linear rheological response of a series of densely branched brush polymers, *Macromolecules* **44**, 6935 (2011).
 - [13] M. Hu, Y. Xia, C. S. Daefler, J. Wang, G. B. McKenna, J. A. Kornfield, and R. H. Grubbs, The linear rheological responses of wedge-type polymers, *J. Polym. Sci., Part B: Polym. Phys.* **53**, 899 (2015).
 - [14] M. Baumgaertel and N. Willenbacher, The relaxation of concentrated polymer solutions, *Rheol. Acta* **35**, 168 (1996).
 - [15] J. Liu, D. Cao, L. Zhang, and W. Wang, Time-temperature and time-concentration superposition of nanofilled elastomers: a molecular dynamics study, *Macromolecules* **42**, 2831 (2009).
 - [16] J. D. Ferry, *Viscoelastic Properties of Polymers*, 3rd ed. (Wiley, New York, 1980).
 - [17] G. B. McKenna, Glass dynamics: Diverging views on glass transition, *Nat. Phys.* **4**, 673 (2008).
 - [18] W. G. Knauss and V. H. Kenner, On the hygrothermomechanical characterization of polyvinyl acetate, *J. Appl. Phys.* **51**, 5131 (1980).
 - [19] D. Pisignano, S. Capaccioli, R. Casalini, M. Lucchesi, P. A. Rolla, A. Justl, and E. Rössler, Study of the relaxation behaviour of a tri-epoxy compound in the supercooled and glassy state by broadband dielectric spectroscopy, *J. Phys.: Condens. Matter* **13**, 4405 (2001).
 - [20] D. J. Plazek, E. Riande, H. Markovitz, and N. Raghupathi, Concentration dependence of the viscoelastic properties of polystyrene-tricresyl phosphate solutions, *J. Polym. Sci., Polym. Phys. Ed.* **17**, 2189 (1979).
 - [21] M. L. Cerrada and G. B. McKenna, Physical aging of amorphous PEN: Isothermal, isochronal and isostructural results, *Macromolecules* **33**, 3065 (2000).
 - [22] H. M. Wyss, K. Miyazaki, J. Mattsson, Z. Hu, D. R. Reichman, and D. A. Weitz, Strain-Rate Frequency Superposition: A Rheological Probe of Structural Relaxation in Soft Materials, *Phys. Rev. Lett.* **98**, 238303 (2007).
 - [23] B. M. Erwin, S. A. Rogers, M. Cloitre, and D. Vlassopoulos, Examining the validity of strain-rate frequency superposition

- when measuring the linear viscoelastic properties of soft materials, *J. Rheol.* **54**, 187 (2010).
- [24] Y. H. Wen, J. L. Schaefer, and L. A. Archer, Dynamics and rheology of soft colloidal glasses, *ACS Macro Lett.* **4**, 119 (2015).
- [25] Y. H. Wen, Y. Lu, K. M. Dobosz, and L. A. Archer, Structure, ion transport, and rheology of nanoparticle salts, *Macromolecules* **47**, 4479 (2014).
- [26] J. Mattsson, H. M. Wyss, A. Fernandez-Nieves, K. Miyazaki, Z. Hu, D. R. Reichman, and D. A. Weitz, Soft colloids make strong glasses, *Nature* **462**, 83 (2009).
- [27] P. Agarwal and L. A. Archer, Strain-accelerated dynamics of soft colloidal glasses, *Phys. Rev. E* **83**, 041402 (2011).
- [28] P. Agarwal, H. Qi, and L. A. Archer, The ages in a self-suspended nanoparticle liquid, *Nano Lett.* **10**, 111 (2010).
- [29] A. R. Jacob, A. S. Poulos, S. Kim, J. Vermant, and G. Petekidis, Convective Cage Release in Model Colloidal Glasses, *Phys. Rev. Lett.* **115**, 218301 (2015).
- [30] A. Philippe, D. Truzzolillo, J. Galvan-Myoshi, P. Dieudonné-George, V. Trappe, L. Berthier, and L. Cipelletti, Glass transition of soft colloids, *Phys. Rev. E* **97**, 040601(R) (2018).
- [31] G. Brambilla, D. El Masri, M. Pierno, L. Berthier, and L. Cipelletti, Probing the Equilibrium Dynamics of Colloidal Hard Spheres Above the Mode-Coupling Glass Transition, *Phys. Rev. Lett.* **102**, 085703 (2009).
- [32] H. H. Winter, M. Siebenbürger, D. Hajnal, O. Henrich, M. Fuchs, and M. Ballauff, An empirical constitutive law for concentrated colloidal suspensions in the approach of the glass transition, *Rheol. Acta* **48**, 747 (2009).
- [33] V. Viasnoff, S. Jurine, and F. Lequeux, How are colloidal suspensions that age rejuvenated by strain application? *Faraday Discuss.* **123**, 253 (2003).
- [34] A. Q. Tool, Relation between inelastic deformability and thermal expansion of glass in its annealing range, *J. Am. Ceram. Soc.* **29**, 240 (1946).
- [35] O. S. Narayanaswamy, A model of structural relaxation in glass, *J. Am. Ceram. Soc.* **54**, 491 (1971).
- [36] C. T. Moynihan, P. B. Macedo, C. J. Montrose, P. K. Gupta, M. A. DeBolt, J. F. Dill, B. E. Dom, P. W. Drake, A. J. Eastaie, P. B. Elterman, R. P. Moeller, H. Sasabe, and J. A. Wilder, Structural relaxation in vitreous materials, *Ann. N. Y. Acad. Sci.* **279**, 15 (1976).
- [37] A. J. Kovacs, J. J. Aklonis, J. M. Hutchinson, and A. R. Ramos, Isobaric volume and enthalpy recovery of glasses. II. A transparent multiparameter model, *J. Polym. Sci., Polym. Phys. Ed.* **17**, 1097 (1979).
- [38] G. B. McKenna, On the physics required for the prediction of long term performance of polymers and their composites, *J. Res. Natl. Inst. Stand. Technol.* **99**, 169 (1994).
- [39] J. C. Dyre, N. B. Olsen, and T. Christensen, Local elastic expansion model for viscous-flow activation energies of glass-forming molecular liquids, *Phys. Rev. B* **53**, 2171 (1996).
- [40] B. Bernstein and A. Shokooh, The stress clock function in viscoelasticity, *J. Rheol.* **24**, 189 (1980).
- [41] T. A. Tervoort, E. T. J. Klompen, and L. E. Govaert, A multi-mode approach to finite, three dimensional, nonlinear viscoelastic behavior of polymer glasses, *J. Rheol.* **40**, 779 (1996).
- [42] S. Jazouli, W. B. Luo, F. Bremond, and T. Vu-Khanh, Application of time-stress equivalence to nonlinear creep of polycarbonate, *Polym. Test.* **24**, 463 (2005).
- [43] R. A. Schapery, Characterization of nonlinear viscoelastic materials, *Polym. Eng. Sci.* **9**, 295 (1969).
- [44] S. Matsuoka, S. J. Aloisio, and H. E. Bair, Interpretation of shift of relaxation time with deformation in glassy polymers in terms of excess enthalpy, *J. Appl. Phys.* **44**, 4265 (1973).
- [45] S. R. Lustig, R. M. Shay, and J. M. Caruthers, Thermodynamic constitutive equations for materials with memory on a material time scale, *J. Rheol.* **40**, 69 (1996).
- [46] J. M. Caruthers, D. B. Adolf, R. S. Chambers, and P. Shrikhande, A thermodynamically consistent, nonlinear viscoelastic approach for modeling glassy polymers, *Polymer* **45**, 4577 (2004).
- [47] D. B. Adolf, R. S. Chambers, J. Flemming, J. Budzien, and J. McCoy, Potential energy clock model: Justification and challenging predictions, *J. Rheol.* **51**, 517 (2007).
- [48] G. A. Medvedev and J. M. Caruthers, A comparison of constitutive descriptions of the thermo-mechanical behavior of polymeric glasses, in *Polymer Glasses*, edited by C. B. Roth (CRC Press, Boca Raton, FL, 2017), Chap. 14, pp. 451–536.
- [49] S. M. Fielding, R. G. Larson, and M. E. Cates, Simple Model for the Deformation-Induced Relaxation of Glassy Polymers, *Phys. Rev. Lett.* **108**, 048301 (2012).
- [50] G. B. McKenna, Mechanical rejuvenation in polymer glasses: Fact or fallacy? *J. Phys.: Condens. Matter* **15**, S737 (2003).
- [51] A. F. Yee, R. J. Bankert, K. L. Ngai, and R. W. Rendell, Strain and temperature accelerated relaxation in polycarbonate, *J. Polym. Sci., Part B: Polym. Phys.* **26**, 2463 (1988).
- [52] F. A. Myers, F. C. Cama, and S. S. Sternstein, Mechanically enhanced aging of glassy polymers, *Ann. N. Y. Acad. Sci.* **279**, 94 (1976).
- [53] H. N. Lee, K. Paeng, S. F. Swallen, and M. D. Ediger, Direct measurement of molecular mobility in actively deformed polymer glasses, *Science* **323**, 231 (2009).
- [54] B. A. Isner and D. J. Lacks, Generic Rugged Landscapes Under Strain and the Possibility of Rejuvenation in Glasses, *Phys. Rev. Lett.* **96**, 025506 (2006).
- [55] Y. G. Chung and D. J. Lacks, How deformation enhances mobility in a polymer glass, *Macromolecules* **45**, 4416 (2012).
- [56] J. Rottler, Local relaxation, aging, and memory of polymer glasses at rest and under stress, in *Polymer Glasses*, edited by C. B. Roth (CRC Press, Boca Raton, FL, 2017), Chap. 11, pp. 375–394.
- [57] P. A. O’Connell and G. B. McKenna, The non-linear viscoelastic response of polycarbonate in torsion: An investigation of time-temperature and time-strain superposition, *Mech. Time-Depend. Mater.* **6**, 207 (2002).
- [58] S. Li, Y. Mi, and X. Wang, Superposed nonlinear rheological behavior in filled elastomers, *J. Rheol.* **61**, 409 (2017).
- [59] J. M. Simmons, A servo-controlled rheometer for measurement of the dynamic modulus of viscoelastic liquids, *J. Sci. Instrum.* **43**, 887 (1966).
- [60] R. I. Tanner, Comparative studies of some simple viscoelastic theories, *Trans. Soc. Rheol.* **12**, 155 (1968).
- [61] L. J. Zapas and A. Wineman, Superposition of small shear deformations on large uniaxial extensions for viscoelastic materials, *Polymer* **26**, 1105 (1985).

- [62] J. Zeegers, D. van den Ende, C. Blom, E. G. Altena, G. J. Beukema, and J. Melema, A sensitive dynamic viscometer for measuring the complex shear modulus in a steady shear flow using the method of orthogonal superposition, *Rheol. Acta* **34**, 606 (1995).
- [63] J. Vermant, L. Walker, P. Moldenaers, and J. Mewis, Orthogonal versus parallel superposition measurements, *J. Non-Newtonian Fluid Mech.* **79**, 173 (1998).
- [64] D. W. Mead, Small amplitude oscillatory shear flow superposed on parallel or perpendicular (orthogonal) steady shear of polydisperse linear polymers: The MLD model, *J. Non-Newtonian Fluid Mech.* **195**, 99 (2013).
- [65] T. G. Mason, Estimating the viscoelastic moduli of complex fluids using the generalized Stokes–Einstein equation, *Rheol. Acta* **39**, 371 (2000).
- [66] M. Baumgaertel, A. Schausberger, and H. H. Winter, The relaxation of polymers with linear flexible chains of uniform length, *Rheol. Acta* **29**, 400 (1990).
- [67] X. Di, X. Peng, and G. B. McKenna, Dynamics of a thermo-responsive microgel colloid near to the glass transition, *J. Chem. Phys.* **140**, 054903 (2014).
- [68] S. Meyer and W. Richtering, Influence of polymerization conditions on the structure of temperature-sensitive poly(N-isopropylacrylamide) microgels, *Macromolecules* **38**, 1517 (2005).
- [69] N. Dingenouts, Ch. Norhausen, and M. Ballauff, Observation of the volume transition in thermosensitive core-shell latex particles by small-angle x-ray scattering, *Macromolecules* **31**, 8912 (1998).
- [70] I. Deike, M. Ballauff, N. Willenbacher, and A. Weiss, Rheology of the thermosensitive latex particles including the high-frequency limit, *J. Rheol.* **45**, 709 (2001).
- [71] H. Senff and W. Richtering, Rheology of a temperature sensitive core-shell latex, *Langmuir* **15**, 102 (1999).
- [72] J.-H. Kim and M. Ballauff, The volume transition in thermosensitive core-shell latex particles containing charged groups, *Colloid Polym. Sci.* **277**, 1210 (1999).
- [73] M. Ballauff, J. M. Brader, S. U. Egelhaaf, M. Fuchs, J. Horbach, N. Koumakis, M. Krüger, M. Laurati, K. J. Mutch, G. Petekidis, M. Siebenbürger, Th. Voigtmann, and J. Zausch, Residual Stresses in Glasses, *Phys. Rev. Lett.* **110**, 215701 (2013).
- [74] D. C. E. Calzolari, I. Bischofberger, F. Nazzani, and V. Trappe, Interplay of coarsening, aging, and stress hardening impacting the creep behavior of a colloidal gel, *J. Rheol.* **61**, 817 (2017).
- [75] X. Peng and G. B. McKenna, Comparison of the physical aging behavior of a colloidal glass after shear melting and concentration jumps, *Phys. Rev. E* **90**, 050301(R) (2014).
- [76] C. P. Royall, W. C. K. Poon, and E. R. Weeks, In search of colloidal hard spheres, *Soft Matter* **9**, 17 (2013).
- [77] X. Peng and G. B. McKenna, Physical aging and structural recovery in a colloidal glass subjected to volume-fraction jump conditions, *Phys. Rev. E* **93**, 042603 (2016).
- [78] T. Eckert and W. Richtering, Thermodynamic and hydrodynamic interaction in concentrated microgel suspensions: Hard or soft sphere behavior? *J. Chem. Phys.* **129**, 124902 (2008).
- [79] G. Romeo, A. Fernandez-Nieves, H. M. Wyss, D. Acierno, and D. A. Weitz, Temperature-controlled transitions between glass, liquid, and gel states in dense p-NIPA suspensions, *Adv. Mater.* **22**, 3441 (2010).
- [80] J. J. Crassous, M. Ballauff, M. Drechsler, J. Schmidt, and Y. Talmon, Imaging the volume transition in thermosensitive core-shell particles by cryo-transmission electron microscopy, *Langmuir* **22**, 2403 (2006).
- [81] U. Gasser, J. S. Hyatt, J.-J. Lieter-Santos, E. S. Herman, L. A. Lyon, and A. Fernandez-Nieves, Form factor of pNIPAM microgels in overpacked states, *J. Chem. Phys.* **141**, 034901 (2014).
- [82] Z. Zhou, J. V. Hollingsworth, S. Hong, G. Wei, Y. Shi, X. Lu, H. Cheng, and C. C. Han, Effects of particle softness on shear thickening of microgel suspensions, *Soft Matter* **10**, 6286 (2014).
- [83] C. A. Angel and K. Ueno, Materials science: Soft is strong, *Nature* **462**, 45 (2009).
- [84] H. Vogel, Temperature dependence of viscosity of melts, *Phys. Z.* **22**, 645 (1921).
- [85] G. S. Fulcher, Analysis of recent measurements of the viscosity of glasses, *J. Am. Ceram. Soc.* **8**, 339 (1925).
- [86] G. Tammann and W. Hesse, Die abhängigkeit der viscosität von der temperatur bei unterkühlten flüssigkeiten, *Z. Anorg. Allg. Chem.* **156**, 245 (1926).
- [87] R. N. Zia, B. J. Landrum, and W. B. Russel, A micro-mechanical study of coarsening and rheology of colloidal gels: Cage building, cage hopping, and Smoluchowski's ratchet, *J. Rheol.* **58**, 1121 (2014).
- [88] B. J. Landrum, W. B. Russel, and R. N. Zia, Delayed yield in colloidal gels: Creep, flow, and re-entrant solid regimes, *J. Rheol.* **60**, 783 (2016).
- [89] M. Fasolo and P. Sollich, Equilibrium Phase Behavior of Polydisperse Hard Spheres, *Phys. Rev. Lett.* **91**, 068301 (2003).
- [90] Y. Zheng, R. D. Priestley, and G. B. McKenna, Physical aging of an epoxy subsequent to relative humidity jumps through the glass concentration, *J. Polym. Sci., Part B: Polym. Phys.* **42**, 2107 (2004).
- [91] S. Banik and G. B. McKenna, Isochoric structural recovery in molecular glasses and its analog in colloidal glasses, *Phys. Rev. E* **97**, 062601 (2018).
- [92] X. Di, K. Z. Win, G. B. McKenna, T. Narita, F. Lequeux, S. R. Pullera, and Z. Cheng, Signatures of Structural Recovery in Colloidal Glasses, *Phys. Rev. Lett.* **106**, 095701 (2011).
- [93] Q. Li, X. Peng and G. B. McKenna, Long-term aging behaviors in a model soft colloidal system, *Soft Matter* **13**, 1396 (2017).
- [94] X. Peng, Microrheology and macrorheology to probe aging of a colloidal glass after volume fraction jumps and shear-melting perturbations, Ph.D. dissertation, Texas Tech University, 2016.
- [95] M. Baumgaertel, M. E. De Rosa, J. Machado, M. Masse, and H. H. Winter, The relaxation time spectrum of nearly monodisperse polybutadiene melts, *Rheol. Acta* **31**, 75 (1992).
- [96] B. Xu and G. B. McKenna, Evaluation of the Dyre shoving model using dynamic data near the glass temperature, *J. Chem. Phys.* **134**, 124902 (2011).
- [97] R. Higler, J. Krausser, J. van der Gucht, A. Zacccone, and J. Sprakel, Linking slow dynamics and microscopic connectivity in dense suspensions of charged colloids, *Soft Matter* **14**, 780 (2018).
- [98] W. van Meegen and S. M. Underwood, The glass transition in colloidal hard spheres, *J. Phys.: Condens. Matter* **6**, A181 (1994).

- [99] T. Shikata and D. S. Pearson, Viscoelastic behavior of concentrated spherical suspensions, *J. Rheol.* **38**, 601 (1994).
- [100] R. H. Ottewill and N. St. J. Williams, Study of particle motion in concentrated dispersions by tracer diffusion, *Nature* **325**, 232 (1987).
- [101] A. Sierou and J. F. Brady, Shear-induced self-diffusion in non-colloidal suspensions, *J. Fluid Mech.* **506**, 285 (2004).
- [102] G. K. Batchelor and J. T. Green, The hydrodynamic interaction of two small freely-moving spheres in a linear flow field, *J. Fluid Mech.* **56**, 375 (1972).
- [103] R. N. Zia and J. F. Brady, in *Complex Fluids in Biological Systems: Experiment, Theory, and Computation*, edited by S. Spagnolie (Springer, New York, 2014), pp. 113–157.
- [104] R. N. Zia, Active and passive microrheology: Theory and simulation, *Annu. Rev. Fluid Mech.* **50**, 371 (2018).
- [105] W. Götze and L. Sjogren, Relaxation processes in supercooled liquids, *Rep. Prog. Phys.* **55**, 241 (1992).
- [106] J. F. Brady, The long time self-diffusivity in concentrated colloidal dispersions, *J. Fluid Mech.* **272**, 109 (1994).
- [107] M. L. Cerrada and G. B. McKenna, in *Time Dependent and Nonlinear Effects in Polymers and Composites*, ASTM STP 1357, edited by R. Schapery and C. Sun (ASTM International, West Conshohocken, PA, 2000), pp. 47–69.